Korean J. Chem. Eng., 37(4), 724-729 (2020)
DOI: 10.1007/s11814-020-0479-4

pISSN: 0256-1115
eISSN: 1975-7220

Experimental and mathematical analysis of electroformed rotating cone electrode

Hamid Heydari, Salman Ahmadipouya, Amirhossein Shoaee Maddah, and Mohammad-Reza Rokhforouz†

Department of Chemical and Petroleum Engineering, Sharif University of Technology, Tehran, Iran
(*Received 12 July 2019 • accepted 5 January 2020*)

Abstract−In this study, we present results of a mathematical model in which the governing equations of electroforming process were solved using a robust finite element solver (COMSOL Multiphysics). The effects of different parameters including applied current density, solution electrical conductivity, electrode spacing, and anode height on the copper electroforming process have been investigated. An electroforming experiment using copper electroforming cell was conducted to verify the developed model. The obtained results show that by increasing the applied current density, the electroforming process takes place faster, thereby resulting in a higher thickness of the electroformed layer. In addition, higher applied current density led to non-uniformity of the coated layer. It was revealed that by increasing electrolytic conductivity from 5 to 20 S/m, the electroformed layer became thicker. By considering three different anode heights, it was found that if the cathode and anode are the same height, the process will be more effective. Finally, it was concluded that there is an optimum value of anode-cathode spacing: above it, energy consumption and plating time are high; while below it, the resultant layer is non-uniform. The present study demonstrates that the developed model can accurately capture the physics of electroforming with a reasonable computational time.

Keywords: Electroforming, Numerical Simulation, Finite Element Method, Thickness Distribution, Rotating Electrode

INTRODUCTION

Electroforming, is an electrochemical process in which deposition of a metallic anode on a different metal cathode by passing a specified current-through a solution takes place. During the past decades, electroforming has been extensively used to manufacture metal parts [1]. It has some advantages over other techniques, including short processing cycle, good copy ability, and high processing precision [2]. Achieving a uniform electroformed layer is a key element in each electroforming process, as it is required in several industries [3-5]. On the other hand, uneven thickness of the electroformed layer could lead to a low-quality product [6,7]. Therefore, it is essential to alleviate the uneven phenomenon to a specified extent. Different techniques have been developed to enhance the thickness uniformity of electroformed layer including secondary cathode [8], rotating electrodes [9], and conformal anode [10]. In addition, by optimization of the process parameters and finding appropriate agitation rate, the uniformity can be improved [11].

Electrochemical cells with a rotating electrode (RE) configuration are mainly designed to impose forced convection on an electrode reaction and simultaneously counteract influences of free convection caused by density and thermal changes in the electrode/electrolyte interface adjacency [12]. It is desirable to obtain homogeneous depositions along the RE surface in the electroforming [13].

Rosales et al. [14] used COMSOL Multiphysics to solve fluid flow equations to simulate turbulent flow in a rotating cylinder electrode reactor (RCE) in a continuous mode of operation. In addition, they solved the averaged diffusion-convection equation in order to achieve residence time distribution. The obtained flow patterns indicate the presence of recirculation zones, and they found that its extent increases with increasing flow rate.

In Pérez and Nava [15], primary, secondary and tertiary current distributions in a rotating cylinder electrode (RCE) using four-plate, six-plate, and concentric cylinder as counter electrodes were computed using finite element method. The influences of electrode rotation speed and applied current density on the distribution of current on RCE cathode were analyzed. The obtained results revealed that homogeneous secondary and tertiary current densities were attainable in the RCE cell. Finally, It was declared that simulation results can be useful in the design of this type of electrochemical.

Currently, no published modeling study has involved electroforming simulation of a rotating cone electrode cell. In this paper, the main objective was to assess the effect of key parameters on the uniformity of the deposited layer. The numerical model equations were solved using a robust finite element solver (COMSOL Multiphysics 5.3a). Electrodeposition experiments using copper electroforming cell validated the numerical simulation of tertiary current distributions. Comparison of experimental and numerical results indicates the accuracy of the developed model. Finally, the effects of applied current density, solution electrical conductivity, electrode spacing, and anode height, on the thickness uniformity are addressed using several sensitivity studies.

MATERIALS AND METHODS

Fig. 1 shows a schematic diagram of an experimental setup built for laboratory studies. The electroforming cell includes the electrolytic solution $CuSO_4 \cdot 6H_2O$ (230 g/L) and concentrated H_2SO_4 (140 g/L), which can enhance the solution conductivity and increase the throwing power of the electrolytic cell. The anodes are 4N pure cop-

†To whom correspondence should be addressed.
E-mail: mrokhforouz92@gmail.com

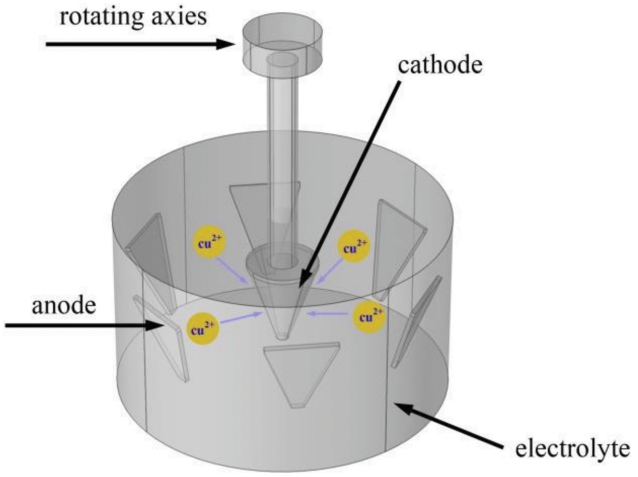

Fig. 1. Schematic diagram of the experimental setup.

per plates placed in a six-plate arrangement, while an aluminum cone with base and top radii of 0.8 and 5 cm, respectively, is used as the substrate on which the copper ions will be deposited. To allow better separation of the electroformed layer from the mandrel, the substrate was treated both chemically and mechanically. The cathode was wired to the direct current via a single copper wire. To improve mechanical and physical properties of the coated electroform layer, the cathode was rotated at 100 rpm. A detailed description of the electrolytic copper cone production can be found elsewhere [16]. Electroplating was conducted in a 4 liter bath with 1.2 V voltage for 48 hr.

GOVERNING EQUATIONS AND BOUNDARY CONDITIONS

Copper electroforming process consists of two steps: copper ion transport from the electrolyte to the cathode surface, and reduction of metal ions by electrochemical reactions on the cathode surface.

It is known that the electrochemical reactions depend on the mass transport and charge transfer when the concentration gradient is significant. Under this circumstance, a tertiary current distribution can be obtained using a Nernst diffusion layer model [17]. A tertiary current distribution model was employed in this work. By considering the concentration boundary layer at the surface of the cathode and diffusion as the dominant mass transfer mechanism, the concentration distribution on the boundary layer was obtained. As the electrolyte is stirred completely outside the boundary layer, the concentration is considered as constant. The critical Reynolds number for a rotating cone electrode is $Re=2\times10^4$. In this study, the Reynolds number is about 3.6×10^4; thus, the assumption of turbulent flow is reasonable. Consequently, in the boundary layer, where the flow is stagnant, the diffusion mechanism is dominant.

Due to this assumption, the results of this work are valid in the case of small rotating speed of electroforming.

Thickness of the boundary layer depends on the electrolyte type, geometry, and agitation rate. It can be estimated using Eisenberg empiric correlation [18]:

Table 1. Variables used for simulation

Parameter	Value (unit)	Symbol
Electrolytic conductivity	12 (S/m)	σ
Cu^{2+} concentration	0.8 (mol/L)	$C_{Cu^{2+},b}$
H_2SO_4 concentration	0.8 (mol/L)	$C_{H_2SO_4}$
Electrolyte density	1,200 (kg/m^3)	ρ
Electrolyte viscosity	0.0012 (Pa·s)	μ
Cu^{2+} diffusion coefficient	5×10^{-10} (m^2/s)	$D_{Cu^{2+}}$
Boundary layer thickness	30×10^{-6} (m)	δ_N
Cell volume	4 (L)	V
Cell temperature	25 (°C)	T
Cathode rotation speed	100 RPM	ω
Exchange current density	0.2 (A/m^2)	i_0
Cathodic current density	4.6 (A/dm^2)	i_c
Relative equilibrium potential (Cu/Cu^{2+})	0 (V)	$E_{eq,rel}$
Anodic potential	0.6 (V)	$\varphi_{s,a}$
Cathodic potential	−0.6 (V)	$\varphi_{s,c}$
Anodic charge transfer coefficient	1.5	α_a
Cathodic charge transfer coefficient	0.5	α_c

$$\delta_N=\frac{r}{0.006Re^{0.91}Sc^{0.356}} \quad (1)$$

where Re denotes the Reynolds number ($Re=\frac{\rho\omega rl}{\mu}=\frac{\rho\omega l^2\sin\alpha}{\mu}$, where ρ is the density, μ is the dynamic viscosity, r is the top radius of the cone, ω is the rotational speed, l is the slant height, and α is the apex half-angle of the cone). In addition, Sc is the Schmidt number ($Sc=\frac{\vartheta}{D}$, where D is the diffusion coefficient and ϑ the kinematic viscosity). The calculated thickness of the diffusion layer is equal to δ_N=30 μm (See Table 1).

In dilute solutions the current density, i_l at any point inside the cell is determined from the gradient of local potential, φ_l according to Ohm's Law:

$$i_l=-\sigma_l\nabla\varphi_l \quad (2)$$

where i_l is the electrolyte current density vector and σ_l is the electrolyte conductivity, which is assumed to be a constant. The potential distribution in the electrolyte was described by the Laplace equation:

$$\nabla^2\varphi=0 \quad (3)$$

Depending on the characteristics of the boundary conditions on the cathode, three types of current distribution models can be specified. When the concentration gradient is significant, the electrochemical reaction is dependent on both the charge transfer and mass transport. For these conditions, a tertiary current distribution was obtained using a Nernst diffusion layer model. The cupric ion concentration within the boundary layer was determined with the Nernst diffusion layer model [17]:

$$\mathbf{N}_i=-D_i\nabla C_i \quad (4)$$

$$\nabla\cdot\mathbf{N}_i=0 \quad (5)$$

where $\mathbf{N}_i$ is the flux of species i, C_i the concentration of the ion i, and D_i the diffusion coefficient.

The concentration at the right boundary of the diffusion layer is set to the bulk concentration:

$$C=C_b \tag{6}$$

To compute the local current density on the cathode surface, the modified Butler-Volmer equation is implemented. This equation requires exchange current density and charge transfer coefficients as input data:

$$i_{loc}=i_0\left[\exp\left(\frac{\alpha_a F\eta}{RT}\right)-\frac{C_{Cu^{2+}\cdot w}}{C_{Cu^{2+}\cdot b}}\exp\left(-\frac{\alpha_c F\eta}{RT}\right)\right] \tag{7}$$

$$\eta=V-\varphi_0 \tag{8}$$

In the above equations, α_a is the anodic charge transfer coefficient, α_c the cathodic charge transfer coefficient, i_o the exchange current density, η the activation overpotential, $C_{Cu^{2+}\cdot b}$ the copper ion concentration in the bulk, $C_{Cu^{2+}\cdot w}$ the copper ion concentration on the cathode surface, and i_{loc} is the local current density. In addition, V is the electrode potential, and φ_0 is the equilibrium potential.

But, at the surface of the anode, the Butler-Volmer equation is used as the boundary condition:

$$i_{loc}=i_0\left[\exp\left(\frac{\alpha_a F\eta}{RT}\right)-\exp\left(-\frac{\alpha_c F\eta}{RT}\right)\right] \tag{9}$$

No-flux boundary conditions were applied for the insulated walls as follows:

$$\mathbf{N}_{Cu^{2+}}\cdot\mathbf{n}=0 \tag{10}$$

Based on the computed local current densities on the surface of the cathode, the locally coated thickness is calculated using Faraday's law:

$$d_{loc}=\frac{i_{loc}tM}{zF\rho} \tag{11}$$

where d_{loc} represents the coating thickness, t is the plating time, z is the number of electrons transferred per ion, M is the atomic weight of copper, and ρ is the density of copper.

Note that the uniformity of the coating distribution (ε) is defined as the ratio of the minimum coating thickness to the average coating thickness.

The electrochemical reaction for the electroforming of copper can be divided into a half-reaction at the anode and cathode, respectively. The deposition at the cathode and the dissolution at the anode are assumed to take place with 100% current yield, which means that the model does not include possible side reactions. The main cathodic reaction is the copper deposition reaction according to:

$$Cu^{2+}(aq)+2e^-\rightarrow Cu(s)$$

And the copper dissolution reaction on the anode surface is represented as:

$$Cu(s)\rightarrow Cu^{2+}(aq)+2e^-$$

MODELING

To perform the simulations, Electrodeposition and Transport of Diluted Species modules of COMSOL Multiphysics were employed [19]. COMSOL Multiphysics, a commercial finite element solver, has been used for electrochemical analysis in several studies during recent years [20-22]. To reduce the computational time, 2D axisymmetric domain was used instead of a 3D geometry since 2D axisymmetric simulations were the only option given computational constraints. Fig. 2 shows the geometry of the constructed model. To measure the coating thickness, the specified blue walls have been selected for thickness measurement.

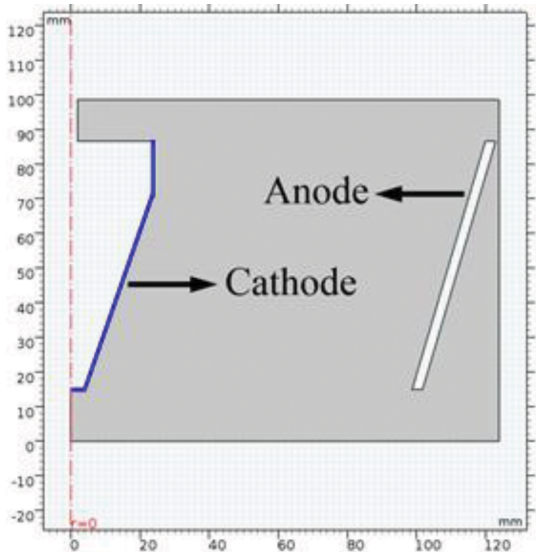

Fig. 2. Schematic view of an axisymmetric geometry. Anode and Cathode are specified with arrows. The red dash-dot line is axisymmetric axis.

Tertiary current distribution is included in the simulation. By considering the concentration boundary layer at the cathode surface and diffusion as the dominant mass transfer mechanism, the concentration gradient in the boundary layer was obtained. As the electrolyte is stirred completely outside the boundary layer, the concentration is considered as constant and independent of the tem-

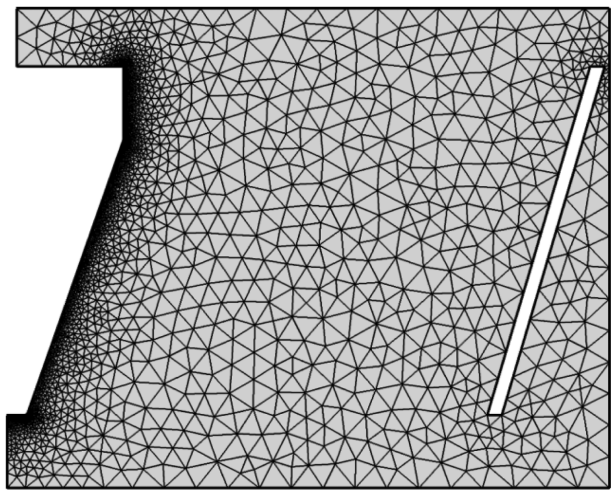

Fig. 3. The discretized domain using mapped and triangular mesh elements.

perature. Consequently, the effects of mass transfer on the current and potential distributions are not included outside the boundary layer. Therefore, by considering that electrical current is constant, current and potential distributions within electrolyte were obtained using secondary current distribution. Since electroforming is a time-dependent process, all simulations were performed as the unsteady-state mode.

The discretized two-dimensional computational domain is illustrated in Fig. 3. As can be seen, mapped mesh elements with extremely refined meshes were employed in the boundary layer; however, triangular mesh elements with fine mesh density were used in the bulk of the system. It is worth noting that refinement of the grids did not produce any significant differences in the results. After the grid independent verification, the numbers of mesh elements were determined as 5,000 and 15,809 in the boundary layer and the bulk of the electrolyte, respectively. The electrolyte properties and the used parameters are given in Table 1.

RESULTS AND DISCUSSION

1. Validation of the Model with Experimental Data

To perform validation of the constructed model, a copper electrodeposition experiment was conducted. The produced conical shell by electroforming method is depicted in Fig. 4. After the process was finished, the electroformed layer was separated from its substrate and then the thickness of the electroformed layer was measured at specified points by using a caliper. The same experimental condition was used in the numerical study. After the model was run, the thickness of the electroformed layer was obtained. Comparison of experimental and numerical coating thickness distribution is illustrated in Fig. 5. As can be seen, there is a good agreement between the results, which shows the model accuracy.

Fig. 4. Conical shell produced by electroforming method.

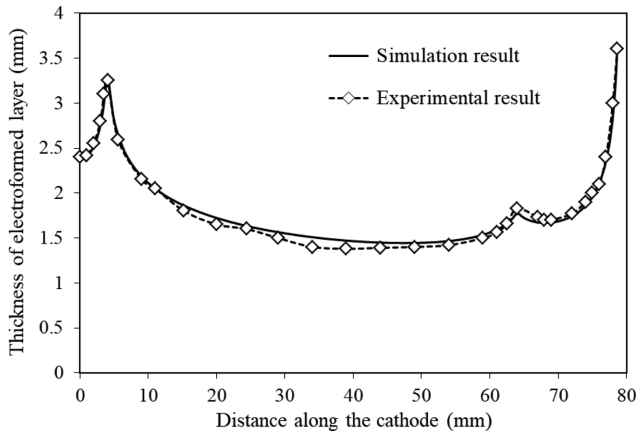

Fig. 5. Comparison of experimental and numerical coating thickness for electroforming in the lab-scale cell in the agitated electrolyte (I=460 A/m^2).

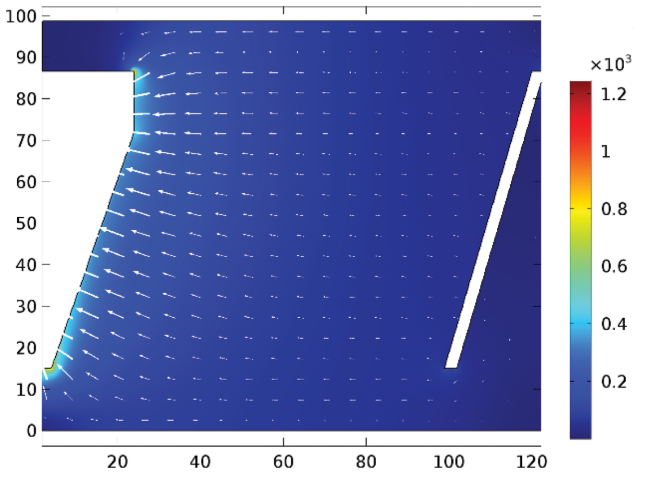

Fig. 6. Electrolyte current density (A/m^2) at t=48 h for the simulated model. In this model, I=460 A/m^2, σ=12 S/m.

Electrolyte current density and velocity fields at t=48 h are shown in Fig. 6. As shown in Fig. 6(a), the current flows from the anode to the cathode. Two high current density zones can be seen at the edges of the cathode surface, which cause non-uniformity of the deposit. Different parameters such as applied current density, and anode-cathode spacing should be adjusted in order to avoid such zones.

2. Sensitivity Analysis

In this section, the effects of operating parameters including current density, solution conductivity, anode height, and anode-cathode spacing on the thickness distribution are investigated using several sensitivity studies.

2-1. Effect of Current Density

Applied current density plays a significant role in the electroforming performance as it controls the amount of electrodeposited layer at the cathode surface. It also affects other factors such as current efficiency and structure of the deposited copper. Additionally, copper plating rate would increase by increasing the current density, but excessive current density results in roughness, and nodular cathode deposits and consequently a low purity copper [23]. Fig. 7 shows the thickness distribution of electroformed layer for different applied current density values of 125, 600, and 850 A/m^2. The electroforming process takes extremely huge process time at the low current density, which is not economical. By increasing applied current density, the electroforming process takes place faster; therefore, it can result in a higher thickness of the electroformed layer. However, higher applied current density leads to non-uniformity

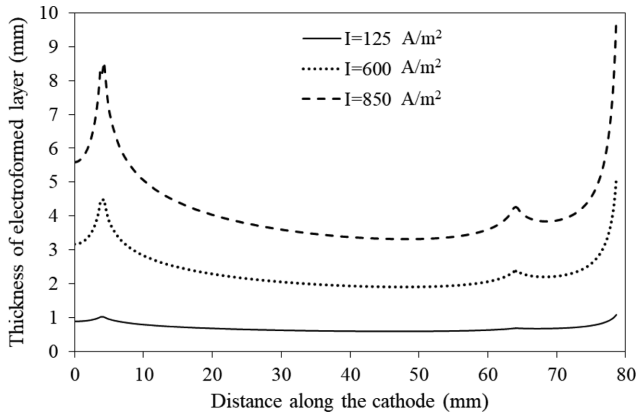

Fig. 7. Thickness of electroformed layer versus distance along the cathode for different applied current densities.

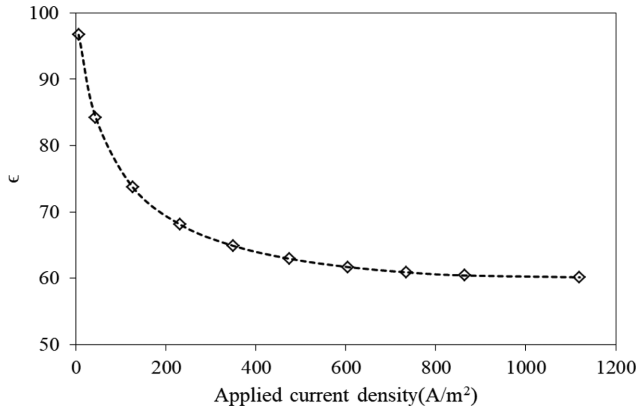

Fig. 8. Variation of coating distribution (ε) as a function of applied current density.

of the coating distribution (shown in Fig. 8). According to this figure, increasing I from 6 to 1,120 A/m^2 leads to reduction of ε by 35%. At higher applied current densities (I>600 A/m^2), increased thickness profile curvature on the top and bottom side of the substrate is observed. It can be concluded that the higher current densities produce spongy-like shape deposits, which is in agreement with experimental observations [24].

2-2. Effect of Conductivity

Electrolytic conductivity (σ), a measure of the solution ability to conduct electricity, is a function of the ion concentration and its type. Conductivity is the reciprocal of the specific resistance. It is known that several physical and chemical phenomena result in conductivity variations. To understand the effect of σ, three different values of 5, 10, 20 S/m were considered (See Fig. 9). The electroformed layer becomes thicker as conductivity increases from 5 to 20 S/m. Higher conductivity, i.e., higher Cu^{2+} concentration, will feed a sufficient and constant amount of Cu^{2+} to the cathode surface, which would enhance the deposition rate and consequently its efficiency. Nevertheless, in a practical application, the increase of electrolyte conductivity or copper ion concentration leads to coarser grains, promoting morphology of the deposited layer into dendritic structure. Our results show that the effect of electrolytic conductivity on the thickness uniformity of the electroformed layer is not considerable. One experiment with σ=10 S/m was conducted to ensure the accuracy of the developed model. As can be seen, there is a good agreement with the experimental and numerical results.

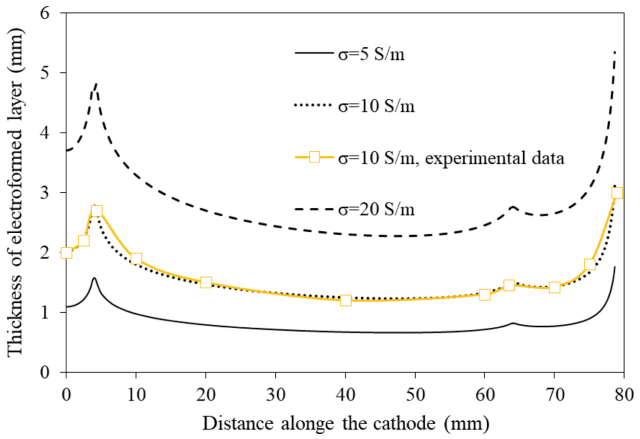

Fig. 9. Thickness of electroformed layer versus distance along the cathode for different solution conductivities.

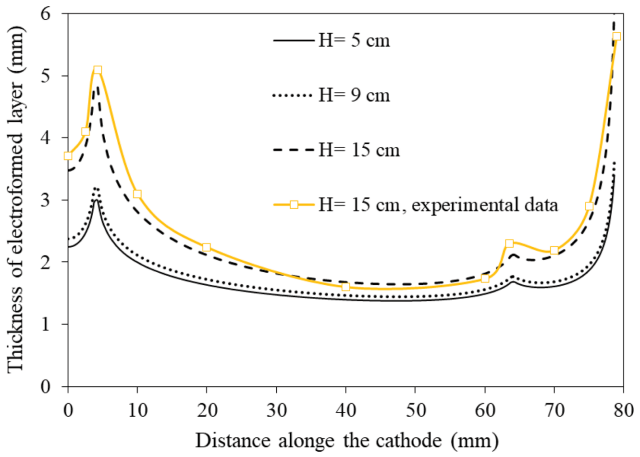

Fig. 10. Thickness of electroformed layer versus distance along the cathode for anode lengths.

2-3. Effect of Anode Height

To understand the impact of anode height (H) on the electroforming process and thickness distribution, three different values of 5, 9, and 15 cm were considered as the height of the anode. The difference between the height of anode and cathode cause accumulation of excess current at the top and bottom of the cathode. When the cathode is much smaller than the anode, the coated layer would be quite non-uniform. In contrast, when they have the same height, a uniform layer would be achieved. Thickness distribution of electroformed layer for different anode heights is presented in Fig. 10. Note that the cathode height is considered as 9 cm in this study. By increasing H from 5 to 9 cm, a marginal increase in the thickness of electroformed layer is observed. It can be observed that further increment of anode height to H=15 cm, results in a thicker layer. But the non-uniformity of the coating distribution will increase drastically (ε=53%). It can be concluded that if the cathode and anode are the same height, the process will be more effective, corresponding to the previous reports [25,26].

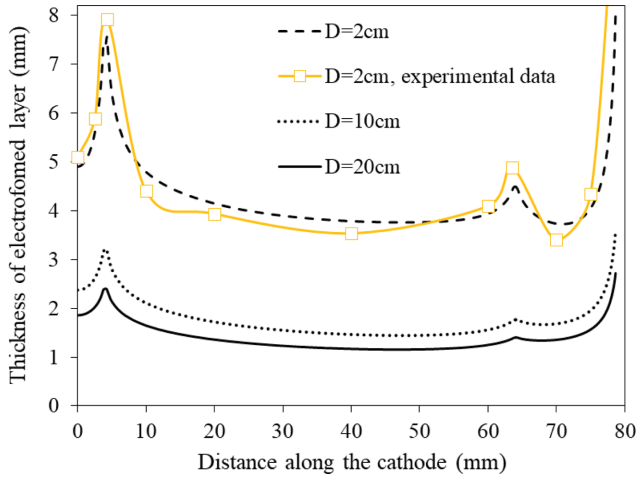

Fig. 11. Thickness of electroformed layer versus distance along the cathode for different anode-cathode spacing.

2-4. Effect of Anode-cathode Spacing

In this part, the effect of anode-cathode spacing on the thickness distribution is quantified. This parameter can affect the energy requirement, recovery efficiency, and quality of the deposit. Thus, the uniformity of the plated surface is strongly dependent on the distance between the two electrodes. Fig. 11 compares thickness distribution of electroformed layer for different anode-cathode spacing. It is clear that increasing the spacing would lead to a decrease in the coated layer thickness and non-uniformity. At D=2 cm, the uniformity is the lowest (ε=60%). While, when the spacing is equal to 10 cm, the resulted layer is more uniform (ε=70%). Thickness of the deposit does not decrease significantly when D reaches to 20 cm. But, that requires higher energy consumption and increase the plating time, which in not economical. Therefore, it is essential to find the optimum value of spacing for each plating process.

CONCLUSION

We assessed the influences of applied current density, solution electrical conductivity, electrode spacing, and anode height on the copper electroforming process. A numerical model was developed and governing equations were solved using finite element method. To validate the model, a conical copper shell was produced by electroforming method, and thickness distribution was compared with the simulation results. Comparison of experimental and numerical results showed that the developed model is accurate enough to capture the qualitative and quantitative nature of the physical process. Our results revealed that using the tertiary current distribution for simulation of the electroforming process is a precise and efficient model and can be used for parametric studies. Performing several sensitivity analyses showed that applied current density and anode height have the highest and lowest impact on the thickness distribution and uniformity of the deposit, respectively. It was observed that increasing the spacing would lead to a decrease in the coated layer thickness and non-uniformity. In addition, higher conductivity, i.e., higher Cu^{2+} concentration, will feed a sufficient and constant amount of Cu^{2+} to the cathode surface which would enhance the deposition rate and consequently its efficiency. Moreover, the obtained results showed that increasing current density resulted in spongy-like shape deposits. The present study demonstrates that computational fluid dynamics can be a reliable approach to optimize the electroforming process.

REFRENCES

1. W. Blum and G. B. Hogaboom, *Principles of electroplating and electroforming*, McGraw-Hill, New York (1949).
2. K. Zhai, L. Du, W. Wang, H. Zhu, W. Zhao and W. Zhao, *Ultrason. Sonochem.*, **42**, 368 (2018).
3. L. Yang, T. Atanasova, A. Radisic, J. Deconinck, A. C. West and P. Vereecken, *Electrochim. Acta*, **104**, 242 (2013).
4. H. Yang and S.-W. Kang, *Int. J. Mach. Tool. Manu.*, **40**, 1065 (2000).
5. T. Kobayashi, J. Kawasaki, K. Mihara and H. Honma, *Electrochim. Acta*, **47**, 85 (2001).
6. J.-d. Li, P. Zhang, Y.-h. Wu, Y.-s. Liu and M. Xuan, *Microsyst Technol.*, **15**, 505 (2009).
7. Y.-J. Tan and K. Y. Lim, *Surf. Coat. Technol.*, **167**, 255 (2003).
8. C.-W. Park and K.-Y. Park, *Results Phys.*, **4**, 107 (2014).
9. D. R. Gabe, *Plat. Surf. Finish.*, **82**, 69 (1995).
10. J.-M. Yang, D.-H. Kim, D. Zhu and K. Wang, *Int. J. Mach. Tool Manu.*, **48**, 329 (2008).
11. H. Z. Pei, J. Zhang, G. L. Zhang and P. Huang, *Adv. Mater. Res.*, **479**, 497 (2012).
12. L. Tong, *Tertiary current distributions on rotating electrodes*, Proceedings of the COMSOL Conference (2011).
13. I. Belov, C. Zanella, C. Edström and P. Leisner, *Mater. Design*, **90**, 693 (2016).
14. M. Rosales, T. Pérez and J. L. Nava, *Electrochim. Acta*, **194**, 338 (2016).
15. T. Pérez and J. L. Nava, *J. Electroanal. Chem.*, **719**, 106 (2014).
16. T. Elshenawy, *Propellants, Explos., Pyrotech.*, **41**, 69 (2016).
17. C. Low, E. Roberts and F. Walsh, *Electrochim. Acta*, **52**, 3831 (2007).
18. M. Eisenberg, C. Tobias and C. Wilke, *J. Electrochem. Soc.*, **101**, 306 (1954).
19. COMSOL Multiphysics, 2017. User's Guide, Version 5.3a. Comsol Inc.
20. E. J. Dickinson, H. Ekström and E. Fontes, *Electrochem. Commun.*, **40**, 71 (2014).
21. E. Sabooniha, M. R. Rokhforouz and S. Ayatollahi, *Oil GasSci. Technol. - Rev. IFP Energies Nouvelles*, **74**, 78 (2019).
22. M. R. Rokhforouz and H. A. Akhlaghi Amiri, *Adv. Water Resour.*, **124**, 84 (2019).
23. A. Shukla and M. Free, *Modeling and measuring electrodeposition parameters near electrode surfaces to facilitate cell performance optimization*, Department of Metallurgical Engineering, University of Utah (2013).
24. T. Elshenawy, S. Soliman and A. Hawwas, *Def. Technol.*, **13**, 439 (2017).
25. N. Obaid, R. Sivakumaran, J. Lui and A. Okunade, *Modelling the electroplating of hexavalent chromium*, COMSOL Conference. Boston2013 (2013).
26. K. C. Pillai, S. J. Chung and I.-S. Moon, *Chemosphere*, **73**, 1505 (2008).